Broadening the Horizons of Fe-Metal in Static Batteries with Anion Exchange Membranes

Lakshya Kumar[1], Hadar Fattal[1], Stav Rahmany[1,2], Hannah Sapir[1], Daniel Mandler[1*], Daniel Sharon[1*], Netanel Shpigel[2*]

[1] Institute of Chemistry, Hebrew University of Jerusalem, Jerusalem 9190401, Israel

[2] Department of Chemical Sciences, Ariel University, Ariel 40700, Israel

1. Experimental section.

1.1 Materials. Iron chloride tetrahydrate [$Fe(Cl)_2.4H_2O$], Potassium ferrocyanide [$K_4Fe(CN)_6$] Nickel(II) chloride [$Ni(Cl)_2$], and Trisodium citrate [$Na_3C_6H_5O_7$] were procured from Thermo Scientific. $LiMn_2O_4$, PVDF (poly (vinylidenefluoride-co-hexafluoropropylene)] and Super P were obtained from Sigma-Aldrich, USA. All other solvents were of analytical grade and purchased from different common suppliers.

1.2 Synthesis of Ni-HCF.

The Ni-HCF was synthesised as reported in a previous article[1] by the gradual addition of $K_4Fe(CN)_6$ to $NiCl_2$ and trisodium citrate in molar ratios of 1:1:1.2, respectively, under vigorous agitation, followed by 24 hours of stirring. Trisodium citrate was synthesised by complete neutralisation of citric acid with sodium hydroxide in 100 mL of deionised water (18.2 MΩ cm), followed by the addition of $NiCl_2$. The solution was agitated for several minutes before the dropwise addition of $K_4Fe(CN)_6$ solution, resulting in the instantaneous formation of a blue precipitate. The suspension was continuously stirred for 24 hours to ensure complete reaction. The solids were isolated by centrifugation at 4000 rpm for 15 minutes, washed alternately with water and ethanol 2–3 times, and subsequently dried at 80 °C under vacuum. The products were pulverised with a mortar and pestle to yield a blue powder.

2. Instrumentation.

Cyclic voltammetry (CV), electrochemical impedance spectroscopy (EIS), and galvanostatic charging and discharging (GCD) measurements were conducted using BioLogic (VSP) instruments. X-ray diffraction patterns were acquired using a Bruker D8 Advance instrument with Cu-Kα radiation.

For sample preparation, X-ray powder diffraction measurements were carried out on a D8 Advance diffractometer with LYNXEYE-XE-T detector (Bruker AXS, Karlsruhe, Germany) operating in

1D mode. Low-background quartz sample holders were carefully filled with the powder samples. XRD patterns within the range °15 to °100 2θ were recorded at room temperature using CuKα radiation (λ=1.5418 Å) with the following measurement conditions: tube voltage of 40 kV, tube current of 40 mA, step-scan mode with a step size of 0.02° 2θ and counting time of 0.5 sec/step. The unit-cell parameters and the crystal structure were refined (Rietveld Quantitative Analysis) using TOPAS, Bruker software.

3. Electrochemical measurements and electrode fabrication.

All electrochemical measurements were performed on a BioLogic potentiostat (VSP-225) at room temperature. The electrochemical performance of all samples was assessed using a typical H-type cell setup, in which Ni-HCF and LMO working electrodes were prepared by mixing a slurry of NiPBA or LMO, conductive carbon (Super P), and PVDF binder in an 80:10:10 weight ratio. Precisely, 80 mg of NiPBA was combined with 10 mg of Super P and 10 mg of PVDF, which were then solubilised in 1-methyl-2-pyrrolidone (NMP) using a mortar and pestle. The resultant slurry was subsequently applied on a 25 μm thick grafoil film functioning as the current collector. The coated film was dried in an oven at 70 °C for several hours until the solvent had evaporated. Subsequently, electrodes were excised from the dried film, and, after adjusting for the mass of the current collector, the active material accounted for approximately 80% of the electrode mass. An iron strip as the counter electrode, and Ag wire as the reference electrode. We conducted a range of electrochemical tests, including CV with iR-compensation, and EIS over a frequency range of 10 mHz to 100 kHz. Additionally, GCD cycles were recorded at different current densities while maintaining constant potential.

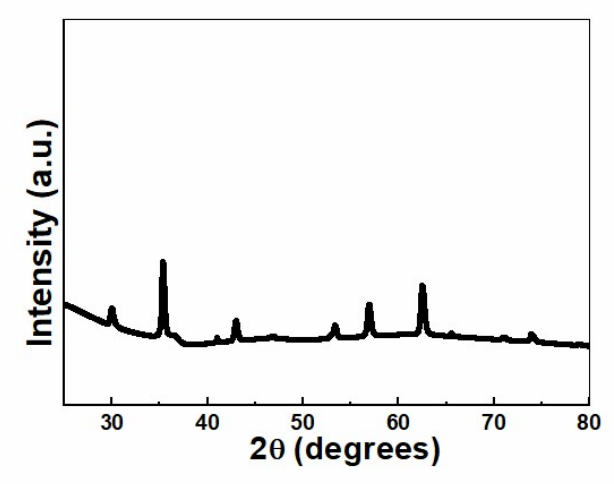

Figure S1: XRD patterns of the Fe anode residue collected from the cell bottom (full cell without AEM) reveal a mixed-phase composition of γ-Fe_2O_3, Fe_3O_4, and Fe_4O_5.

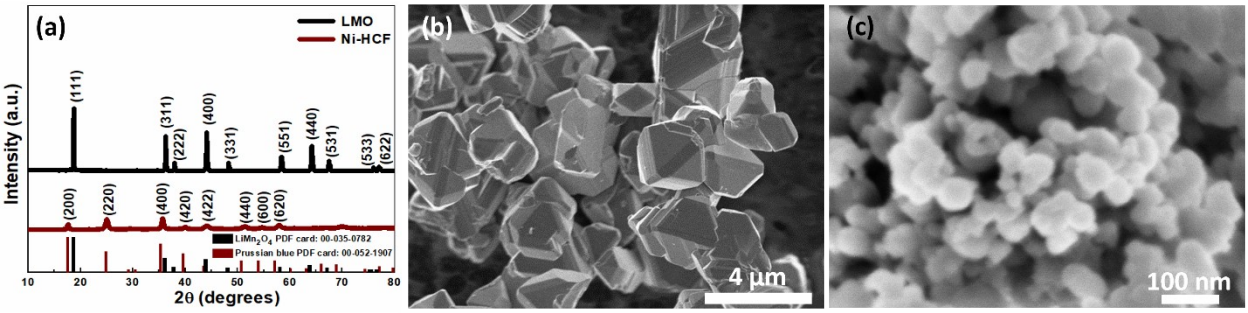

Figure S2: (a) XRD patterns of as-prepared LMO and Ni-HCF and standard XRD patterns (black and brown curves). (b) FE-SEM images of the LMO and Ni-HCF samples, respectively.

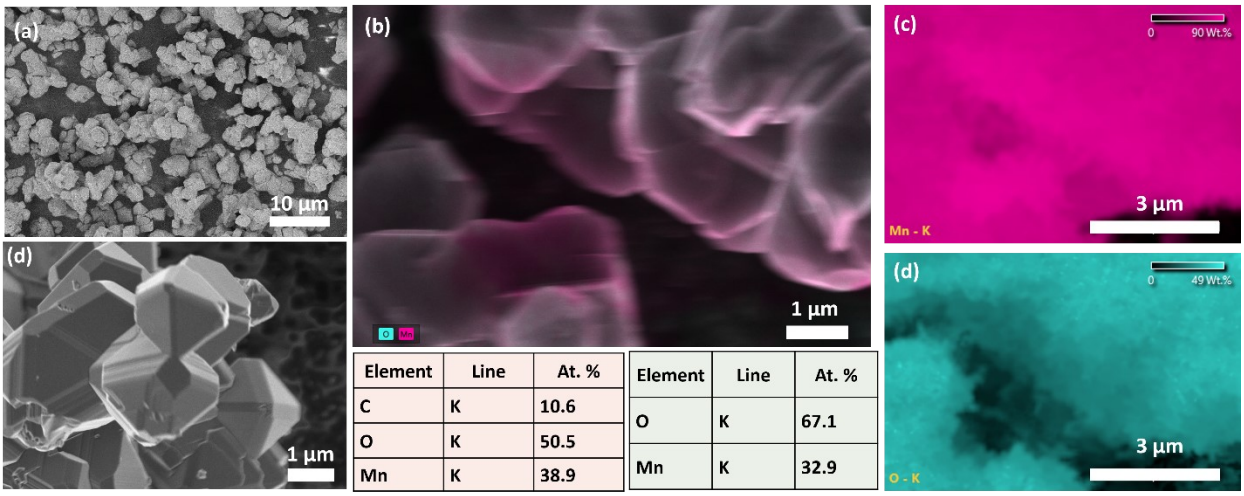

Element	Line	At. %
C	K	10.6
O	K	50.5
Mn	K	38.9

Element	Line	At. %
O	K	67.1
Mn	K	32.9

Figure S3: (a, d) FE-SEM images of the LMO sample at different magnifications. (b, c, d) EDX analysis of the LMO sample. The inset table in Figure b shows the elemental atomic percentages.

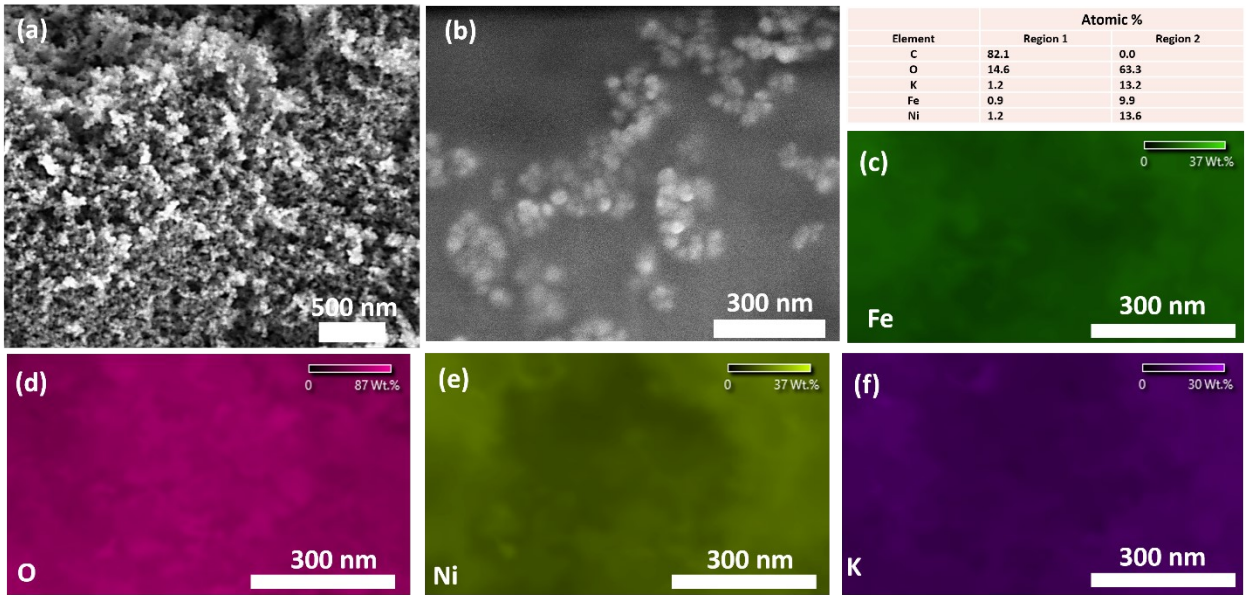

	Atomic %	
Element	Region 1	Region 2
C	82.1	0.0
O	14.6	63.3
K	1.2	13.2
Fe	0.9	9.9
Ni	1.2	13.6

Figure S4: (a, b) FE-SEM images of the Ni-HCFsample at different magnifications. (c, d, and f) EDX analysis of the Ni-HCF sample. The table in the above Figure c shows the elemental atomic percentages.

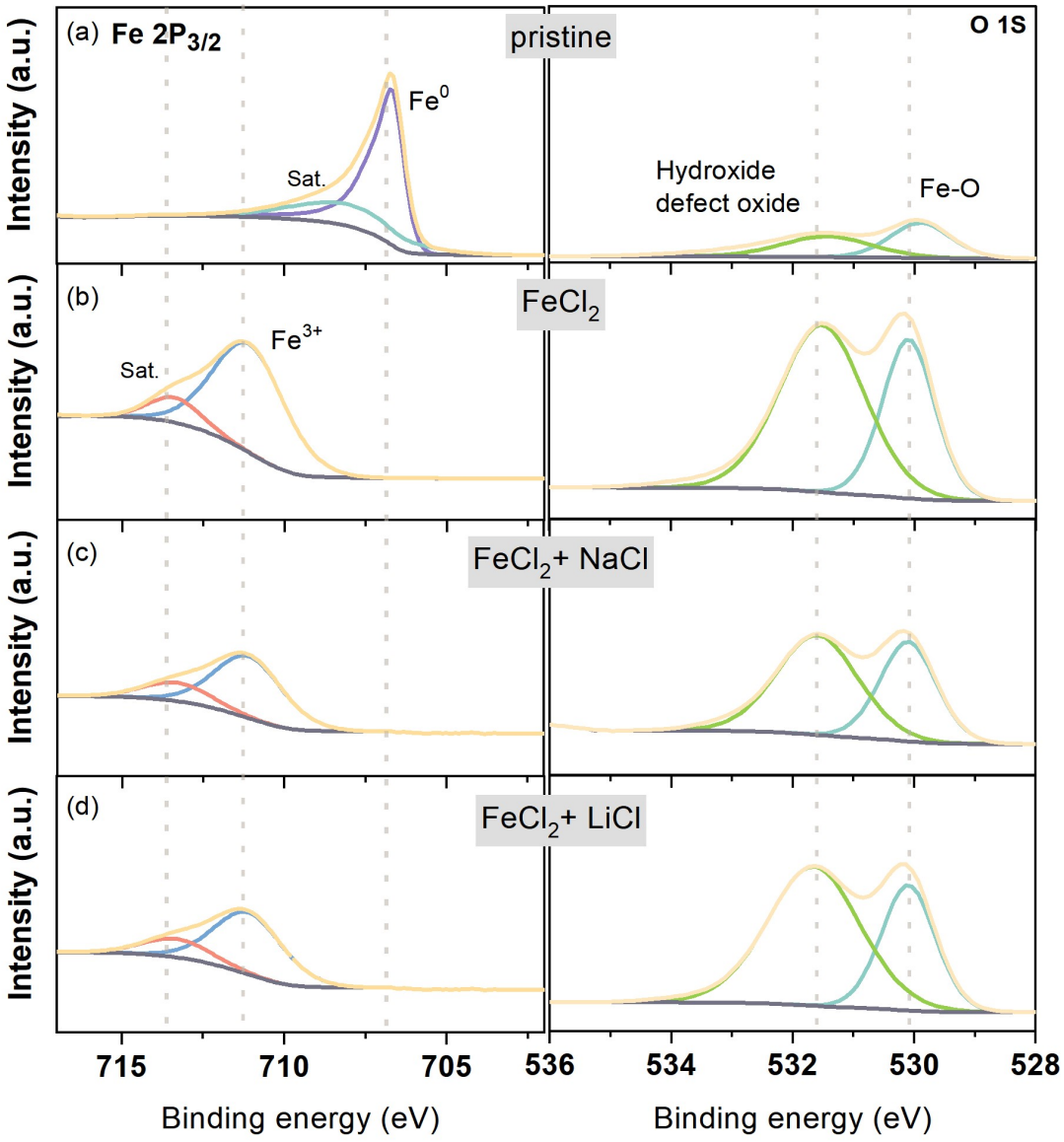

Figure S5 XPS spectra of the Fe $2p_{3/2}$ and O 1s regions for **(a)** pristine iron foil and for iron electrodes after cycling in **(b)** 1 M $FeCl_2$, **(c)** 1 M $FeCl_2$ + 4 M NaCl, and **(d)** 1 M $FeCl_2$ + 4 M LiCl electrolytes

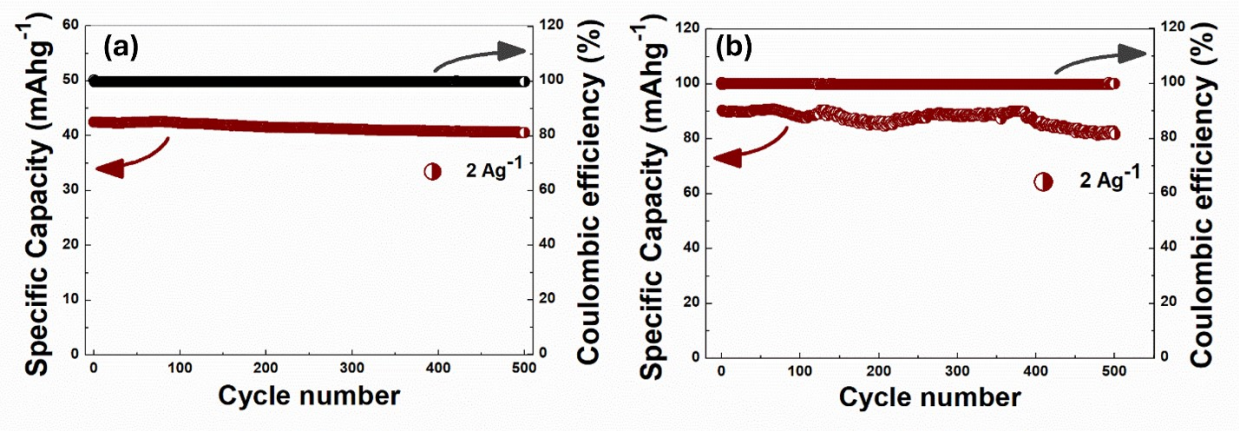

Figure S6: (a, b) Specific capacity and coulombic efficiency of the Ni-HCF and LMO half-cells over 500 charge–discharge cycles.

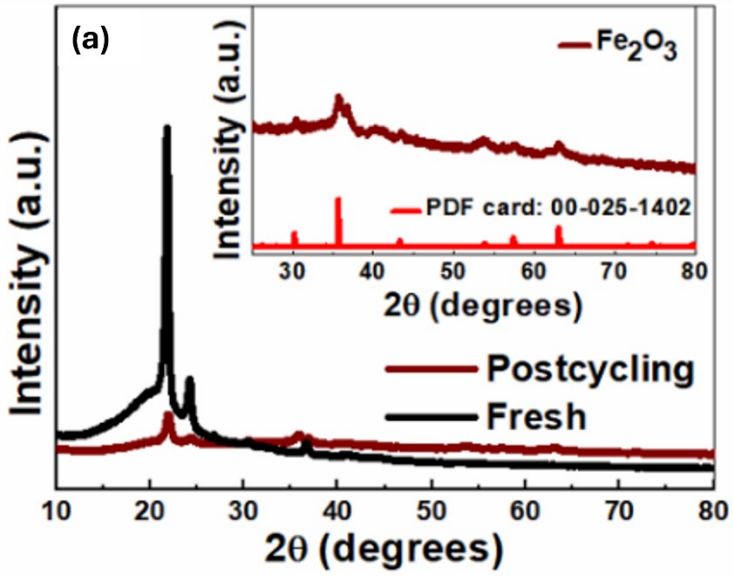

Figure S7: XRD patterns of the AEM on the iron side before and after cycling; inset highlights Fe_2O_3 formation after 1000 cycles.

References:

1. G. Gavriel, B. Bergman, M. Turgeman, A. Nimkar, Y. Elias, M. D. Levi, D. Sharon, N. Shpigel and D. Aurbach, *Mater. Today Energy*, 2023, **31**, 101189.